Int. J. Electrochem. Sci., 11 **(2016)** 7705 – 7713, doi: 10.20964/2016.09.14

International Journal of
ELECTROCHEMICAL
SCIENCE
www.electrochemsci.org

Electrodeposition of Poly(sodium 4-Styrenesulfonate)-Silver Nanocomposites for Electrochemical Detection of H_2O_2

Qingbin Guo[*], *Meixia Li*

Hebei University of Engineering, Handan, Hebei, 056038, P.R. China
[*]E-mail: qingbinguo_hun@yeah.net

Received: 27 May 2016 / *Accepted:* 13 July 2016 / *Published:* 7 August 2016

A polystyrene sulphonic acid-silver nanocomposite (PSS-Ag NPs) using $AgNO_3$-PSS solution as precursor was successfully deposited on the glassy carbon electrode (GCE) via electrodeposition. The prepared PSS-Ag NPs/GCE was then applied as active electrode material of non-enzymatic electrochemical sensors for H_2O_2 detection. The performance of PSS-Ag NPs/GCE for electrocatalytic reduction of H_2O_2 was better than that of Ag NPS/GCE and PSS/GCE electrode. The linear response ranging of the sensor with PSS-Ag NPs modified electrode was from 1.5 μM to 2.0 mM. And the detection limit was 0.7 μM (S/N = 3). Owing to the outstanding electrocatalytic activity and rapidly electron transport property of PSS-Ag NPs composite, the non-enzymatic H_2O_2 sensor constructed with PSS-Ag NPs/GCE was highly stable and sensitive.

Keywords: Polystyrene sulphonic acid; Silver nanoparticles; H_2O_2; Electrodeposition; Sensor

1. INTRODUCTION

Hydrogen peroxide, chemically known as H_2O_2, has become one of the most important commercial chemicals owing to its widely used in various fields such as paper and pulp industry, pharmaceutical and healthcare, food process, minerals process and chemical production process ADDIN EN.CITE [**Error! Bookmark not defined.**. In the biological events, H_2O_2 is involved in the process as the by-product of oxidases such as D-amino acid oxidase, alcohol oxidase, glucose oxidase and oxalate oxidase. Besides, H_2O_2 can also participate as a substrate in the reaction catalyzed by enzyme horseradish peroxidase. In the production of varieties of organic compounds, H_2O_2 has long been used as strong oxidizing agent. Moreover, H_2O_2 can be employed as oxidant in liquid-based fuel cells due to its oxidizing ability [1, 2]. In all applications mentioned above, the determination of H_2O_2 is of great importance, leading to the intensively study of developing a determination method with high efficiency, highly sensitive and low cost recently. Till now, several techniques such as

chromatography, spectrophotometry, fluorescence and phosphorescence have been employed. However, almost all methods exhibited certain shortcomings including susceptibility to disturbances, time consuming or high cost [3]. Electrochemical sensors, a newly developed technique with many advantages (e.g., fast response, simplicity and high sensitivity), have demonstrated its potential for detecting H_2O_2 accurately and sensitively. [4]. Recently, designing and producing novel sensors for determination of H_2O_2 has attracted intensive research interest.

To improve the performance of H_2O_2 sensor (e.g., sensitivity, selectivity and stability), the crucial factor is the immobilization of heme proteins on the surface of electrodes. Various methods including entrapment, crosslinking, covalent linking and adsorption have been explored for the immobilization of biomolecules. As to the matrix used for immobilization, a variety of materials including sol-gel materials, polymers, nanomaterials, surfactants and biomaterial (e.g., chitosan, cellulose, DNA, eggshell membrane and fibroin[5][6][6][9][9][9][9][9][9][9]) [6] have been reported. Among all mentioned materials, nanomaterials especially metal nanoparticles were most studied and experienced a vigorous development as a matrix for immobilization.

Along with the development of basic nanoscience, metal nanoparticles with unique optical, electrical, thermal and catalytic properties have attracted worldwide attention. Metal nanoparticles have successfully applied to various areas such as nanosensors, biomedicine, catalysis and microelectronics [7]. As a promising matrix used for immobilization of proteins, metal nanoparticles possess many unique properties such as favorable biocompatibility, high catalytic activity and excellent electric conductivity, which is highly beneficial for the improvement of sensor performance [8].

Among the reported metal nanoparticles, silver nanoparticles (Ag NPs) has long been concerned by researchers due to their catalytic properties [9, 10]. Therefore, Ag NPs are generally used as catalysts in a large number of reactions. Except its catalytic performance, Ag NPs still own many other attractive properties. For example, Ag NPs can effectively promote surface enhanced optical phenomena. Besides, the well-known antibacterial properties and excellent electrical and thermal conductivity are also fascinating [11, 12]. As revealed by Campbell et al. [13], the reduction of H_2O_2 could occur at an Ag NP array. The voltammetric trace in the process of H_2O_2 reduction was influenced by the size and surface coverage of nanoparticles. Both the decrease of size or surface coverage of nanoparticles will lead to a negative shift of peak potential. Besides, Ward Jones et al. have simulated the effects of the size of Ag NPs on the anodic stripping voltammetry and the obtained simulation results were compared with experimental data [14]. Furthermore, it is very advantageous to combine the polymers and Ag NPs together. The addition of Ag NPs not only strengthens the polymer but enhances the electrical property through the synergistic reaction between the polymer and Ag NPs. When the size of doped metals in the polymer was reduced to nanoscale, the conducting performance of the obtained composite further increased [15-19]. Besides, for the nanocomposites, the electrocatalytic reactivity also increased with the decreasing size of materials [20, 21]. On the other hand, the aggregation of doped nanoparticles can be prevented by the surrounding polymers, and the acquired easing of the electron transfer has resulted in the increase of the sensitivity and selectivity [22].

A large number of preparation methods for the composite contained Ag NPs and polymer have been reported nowadays. However, the complicated process hindered the industrial applications. Therefore, the development of a simple and low-cost fabrication method for the polymer-Ag NPs composite was highly demanded. In our work, a composite of poly (sodium 4-Styrenesulfonate) (PSS) and Ag NPs was prepared by electrochemical deposition and the obtained composite was applied in the construction of a high sensitive H_2O_2 sensor. The morphology and chemical composition of the composite was measured by SEM and EDX. Besides, the electrocatalytic reactivity of the Ag nanoparticles doped PSS polymer was investigated in details.

2. EXPERIMENTS

2.1. Materials

Poly(sodium 4-styrenesulfonate) (average Mw ~1,000,000), silver nitrate (99%), ammonia solution and were purchased from Sigma-Aldrich and used without further purification. A stock solution was diluted to prepare the hydrogen peroxide solution, which was prepared exactly before the use in order to avoid the decomposition. Standard solutions of Na_2HPO_4 and NaH_2PO_4 were mixed to prepare the phosphate buffer solutions (PBS). Pure water was obtained by passing through Milli-Q water purification set.

2.2. Electrodeposition and electrochemical determination

To prepare the silver-ammonia $[Ag(NH_3)_2OH]$ solution, the ammonia (1 wt%) was gradually added into the silver nitrate solution (50 mM). When the precipitates were completely dissolved, the solution of silver-ammonia $[Ag(NH_3)_2OH]$ with the concentration of around 40 mM was acquired [23]. 2 mL of PSS solution (10 mM) was added into 8 mL of the prepared $Ag(NH_3)_2OH$ solution. Then the PSS-Ag NPs nanocomposite was electrodeposited on the glassy carbon electrode (GCE) by amperometric method. Three-electrode cell (glassy carbon as working electrode, saturated calomel as reference electrode and platinum as counter electrode) was used. The experiment was carried out at under high-purity nitrogen atmosphere and the voltage was set at 1 V for 30 s using a potentiostat/galvanostat (PGSTAT-302N, Autolab). Then the modified electrode was transferred to 0.1 M phosphate buffer solution without monomer, and cyclic voltammetry technique was explored to eliminate residual monomers and oligomers. The potential was set ranging from 0 to 0.8 V with the scan rate 50 mV/s. The EIS measurements were also conducted. The frequency was from 10 mHz to 100 kHz and the signal amplitude was 5 mV around the open circuit potential with 10 points was acquired per decade. Then the nonlinear least-square fitting procedure was applied to fit the obtained EIS data to equivalent circuits with the chi-squared value minimized to 10^{-4}.

2.3. Characterizations

The structure of Au nanoparticles was measured by means of XRD (PW3040/60 X'pert PRO) with the data collected from 10° to 80°. The morphology and compositions of the prepared PSS-Ag

NPs composite were characterized by field emission scanning electron microscopy (FESEM Quanta 200F) coupled with energy dispersive X-ray (EDX) spectroscopy. To prepare the sample for SEM and EDX test, the composite was firstly dispersed in water with mild ultrasound, then 0.01 ml of the prepared suspension was dropped on the well-polished silicon surface and dried at room temperature.

3. RESULTS AND DISCUSSION

Fig.1 depicted the SEM image of the prepared PSS-Ag NPs composite by electrodeposition and the size distribution diagram of the doped Ag nanoparticles. As can be seen form Fig. 1, the spherical Ag NPs with average size of 26.72 nm was dispersed homogeneously without agglomeration in the PSS-Ag NPs nanocomposite.

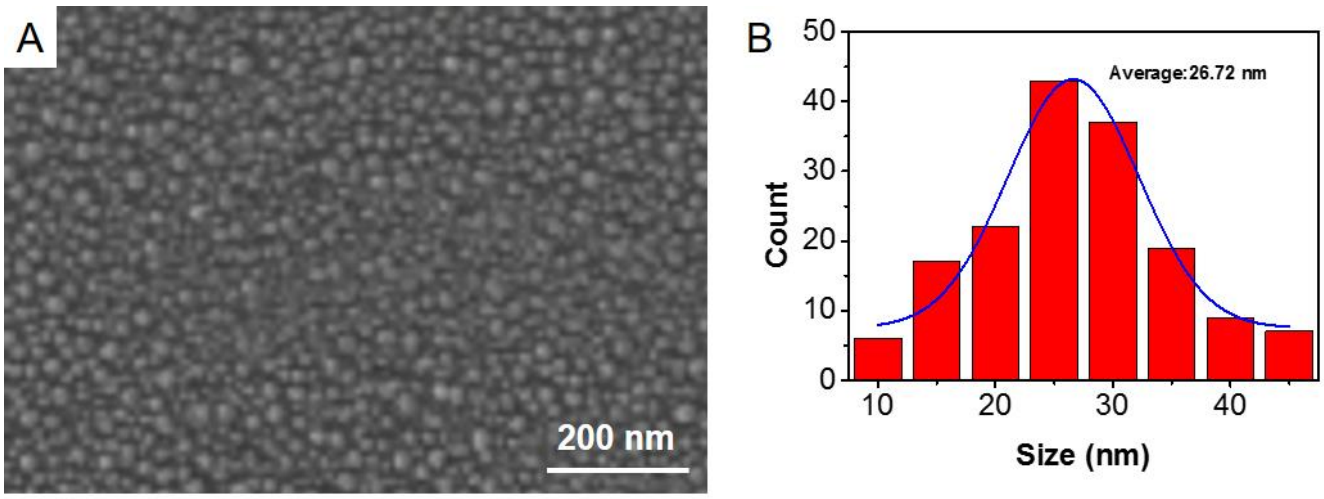

Figure 1. (A) SEM image and (B) size distribution diagram of PSS-Ag NPs composite prepared by using electrodeposition.

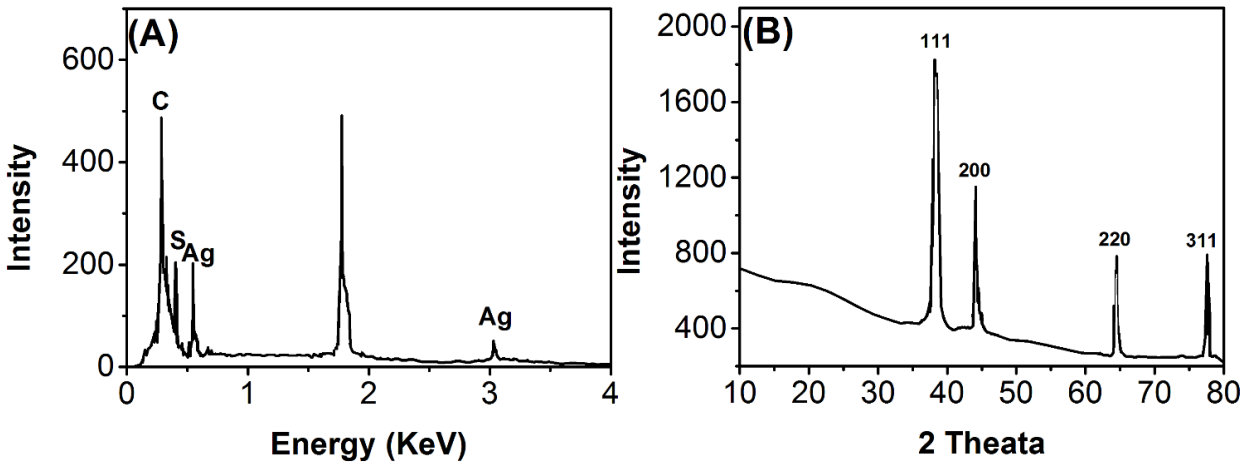

Figure 2. (A) EDX spectrum and (B) XRD pattern of PSS-Ag NPs composite.

Energy-dispersive X-ray spectroscopy (EDX) was used to estimate chemical composition of PSS-Ag NPs composite and the results was shown in Fig. 2A. The Ag peak from the Ag NPs and the C and S peaks from PSS can be clearly observed, indicating the successful synthesis of the PSS-Ag NPs composite. The structure of the PSS-Ag NPs composite was characterized by XRD (Fig. 2B). Relatively marginal peaks at lattice planes of 111, 200, 220, and 311 were observed, which confirmed that the doped Ag nanoparticles were not in the Ag^+ form.

Ag NPs have been reported to demonstrate high electrocatalytic activity for the reduction of H_2O_2. For the sake of evaluating the electrochemical performance of Ag NPs, the electrocatalytic activity of Ag NPS/GCE, PSS/GCE and PSS-Ag NPs/GCE was investigated by cyclic voltammetry. The experiments were carried out in a 0.1 M phosphate buffer solution at pH 6.5 with or without 1 mM H_2O_2 at a scan rate of 50 mV/s. As shown in Fig. 3A, in the presence of hydrogen peroxide, no electrochemical activity was shown with the PSS/GCE at the selected potential range, while the PSS-Ag NPs/GCE had showed an outstanding electrocatalytic performance toward H_2O_2 reduction. Besides, the reduction peak current of Ag NPS/GCE was less than that of PSS-Ag NPs/GCE. Under the condition of no H_2O_2, a little reduction peak at about —0.2 V was found on PSS-Ag NPs/GCE. However, the reduction peak increased rapidly after the addition of H_2O_2, suggesting the high performance of PSS-Ag NPs/GCE for electrocatalytic reduction of H_2O_2. In all, it can be speculate that the synergistic effect between Ag NPs and PSS have greatly improved the performance of PSS-Ag NPs/GCE for electrocatalytic reduction of H_2O_2.

The equations involved in electrocatalytic reduction of H_2O_2 by PSS-Ag NPs composite was listed as follows:

$$2\text{PSS-Ag NPs(0)} + H_2O_2 \rightarrow 2\text{PSS-Ag NPs(I)-OH}$$

$$2\text{PSS-Ag NPs(I)-OH} + 2H^+ + 2e^- \rightarrow 2\text{PSS-Ag NPs(0)} + 2H_2O$$

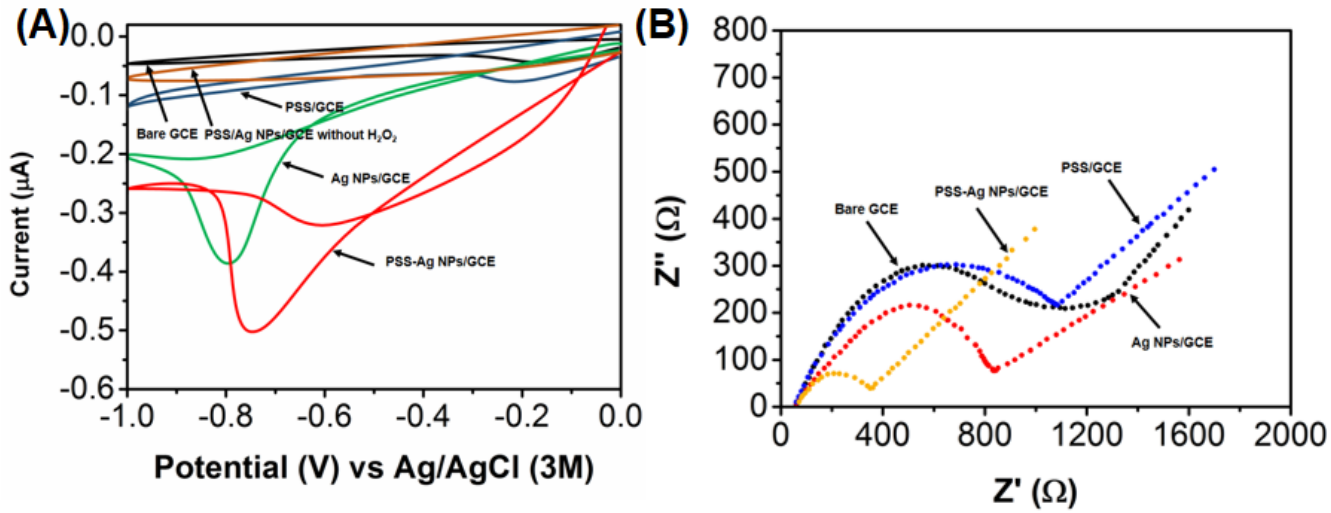

Figure 3. (A) Cyclic voltammograms of GCE, PSS/GCE, Ag NPs/GCE and PSS-Ag NPs/GCE in the presence of 1 Mm H_2O_2 (B) Nyquist diagrams of electrochemical impedance spectrum of GCE, PSS/GCE, Ag NPs/GCE and PSS-Ag NPs/GCE.

Electrochemical impedance spectroscopy (EIS) was employed to investigate the impedance changes of the modified electrode. The Nyquist plots obtained in 0.1 M KCl solution containing 1 mM $Fe(CN)_6^{3-/4-}$ was shown in Fig. 3B. The Nyquist plot of impedance spectra contained two parts: a line at lower frequencies related to the diffusion process and a semicircle at higher frequencies related to the electron transfer limited process. A smaller semicircle was observed at PSS-Ag NPs/GCE compared with bare GCE, PSS/GCE and Ag NPs/GCE, indicting the decrease of the electron-transfer resistance owing to the synergistic action of Ag NPs and PSS. According to the cyclic voltammetry and EIS tests, the remarkable enhancement of electrocatalytic property of the PSS-Ag NPs/GCE was confirmed.

The typical amperometric response curves of 0.1 mM H_2O_2 in PBS with pH 7.8 was recorded at the applied voltage of —0.72 V on Ag NPs/GCE and PSS-Ag NPs/GCE, and the results were shown in Fig. 4A. The current response of PSS-Ag NPs/GCE was about 5.41 times higher than that of Ag NPs/GCE. A fast and well-defined linear amperometric response could be observed on PSS-Ag NPs/GCE. However, a deviation occurred at high concentrations, probably because that the existence of large amount of hydrogen peroxide resulted to the leading role of chemical oxidation of the reduced modifier [24]. The calibration curve for H_2O_2 sensor was shown in Fig.4B. The current response was related linearly with the concentration of H_2O_2 ranging from 1.5 μM to 2.0 mM. And the detection limit of the sensor was 0.7 μM (S/N = 3). The sensitivity of the PSS-Ag NPs/GCE was compared with that of other reported Ag NPs modified electrodes and the results were presented in Table 1. Obviously, the PSS-Ag NPs/GCE showed the highest sensitivity owing to the doping of Ag NPs nanoparticles to PSS, which effectively enhanced electron transfer between Ag NPs and PSS and increased the electrocatalytic active area [25].

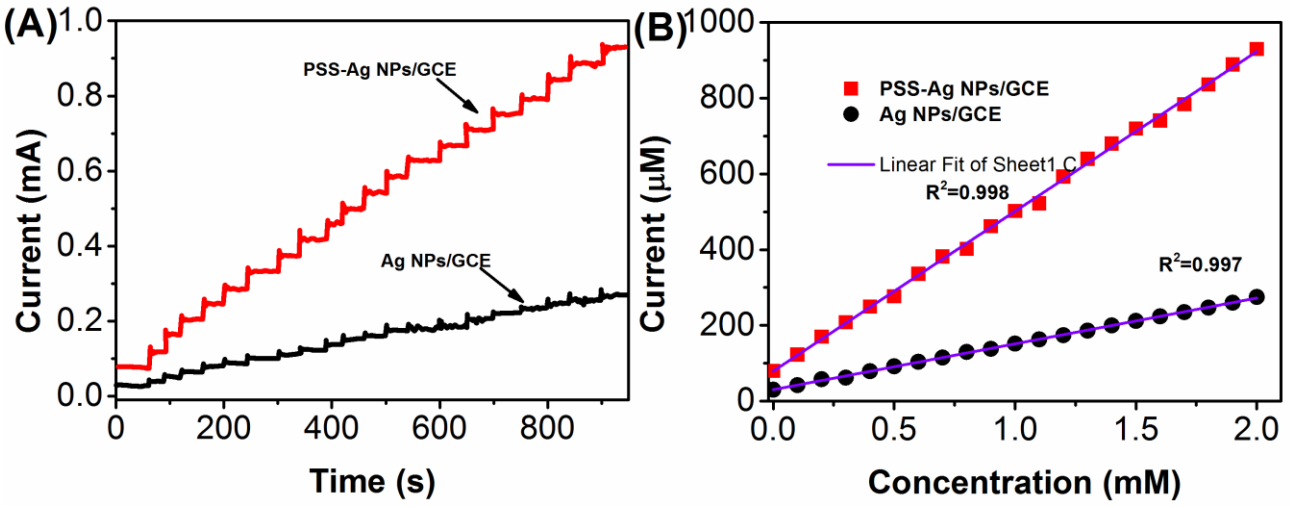

Figure 4. (A) Current–time response obtained on increasing the glucose concentration in 0.10 mM steps at the PSS-Ag NPs/GCE and Ag NPs/GCE VACNTs. (B) The dependence of the current response verses the concentration of H_2O_2 at the PSS-Ag NPs/GCE and Ag NPs/GCE.

The reproducibility and stability are two important factor for electrochemical sensors. The amperometric current responses from five PSS-Ag NPs/GCE nanocomposite electrodes were obtained at the potential of -0.72 V.

Table 1. Comparison of the present PSS-Ag NPs/GCE sensor with other H_2O_2 sensors.

Electrode	Linear detection range	Detection limit	Reference
Ag NPs/ZnO/GCE	0.22 mM to 5.5 mM	0.042 mM	[26]
Cu NPs-CuHCF/ PEDOT/GCE	1 mM to 5.4 mM	0.1 mM	[27]
Hb/C@Au	5 mM to 13.5 mM	0.167 mM	[28]
MnO_2/nafion/GCE	0.01 mM to 0.15 mM	0.002 mM	[29]
Cryptomelane-type manganese oxides/CPE	0.1 mM to 0.69mM	0.002 mM	[30]
PSS-Ag NPs/GCE	0.1 mM to 2.0 mM	0.02 μM	This work

The relative standard deviation (RSD) of obtained results was 3.7%, suggesting the reproducibility of the prepared PSS-Ag NPs/GCE. Furthermore, six measurements with 1 mM H_2O_2 were carried out on the same PSS-Ag NPs/GCE, and the RSD value of obtained results was found to be 1.9%, indicating the stability of the sensor. Moreover, the long-term stability of the sensor was also investigated by exposing the sensor to air and testing every 2 days. As can be seen from Fig. 5, the current response remained 87% of its original data after 30 days, probably resulting from the chemical stability of PSS-Ag NPs in air.

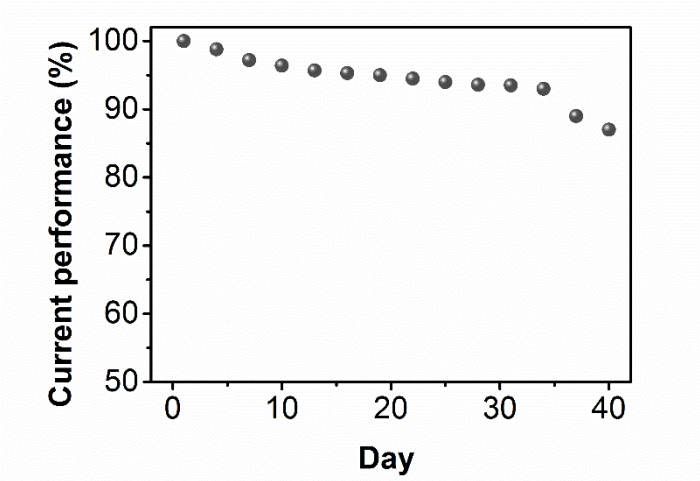

Figure 5. Long-term stability of the PSS-Ag NPs/GCE at room temperature.

In an attempt to explore the PSS-Ag NPs composite for field application, the fabricated sensor was used for determining H_2O_2 in supermarket purchased milk. In a typical process, 250 μL milk sample was added into 10.0 mL 0.2 M PBS. The current value was then recorded at ―0.72 V. Table 2 illustrates the results of the determinations. The H_2O_2 concentration in two milk samples is 0.2

mM and 0.5 mM, respectively. The recovery performance of H_2O_2 was deduced using standard addition method. It can be seen that the PSS-Ag NPs/GCE shows excellent recovery values. Titanium sulfate colorimetric method was used as a comparison technique for determine the value of H_2O_2 [31], which suggests the PSS-Ag NPs composite is an excellent analytical candidate for H_2O_2 determination.

Table 2. Determination of H_2O_2 in milk samples using amperometry and control method.

Sample	H_2O_2 value	Added	Found	RSD	Recovery	Titanium sulfate colorimetry
1	0.2 mM	0.1 mM	0.305 mM	3.11%	101.67%	0.296 mM
2	0.5 mM	0.2 mM	0.727 mM	2.54%	103.86%	0.722 mM

4. CONCLUSIONS

In this study, the PSS-Ag NPs composite was successfully synthesized by a one-step electrodeposition. The Ag NPs was dispersed homogeneously in PSS matrix. The as-prepared PSS-Ag NPs/GCE was investigated for electrochemical determination of H_2O_2. The performance obtained on the PSS-Ag NPs/GCE was much better than that obtained on the Ag NPs/GCE. More important is that the prepared PSS-Ag NPs/GCE has demonstrated promising potential for determination of H_2O_2 in milk sample.

ACKNOWLEDGEMENTS
This work was financially supported by National Natural Science Foundation of China (No. 51541403) and Natural Science Foundation of Hebei Province (No. E2014402106).

References

1. J.B. Raoof, R. Ojani, E. Hasheminejad and S. Rashid-Nadimi, *Appl. Surf. Sci.*, 258 (2012) 2788
2. A. Salimi, R. Hallaj, S. Soltanian and H. Mamkhezri, *Anal. Chim. Acta.*, 594 (2007) 24
3. H. Razmi, R. Mohammad-Rezaei and H. Heidari, *Electroanalysis*, 21 (2009) 2355
4. Y. Liu, D. Wang, L. Xu, H. Hou and T. You, *Biosensors and Bioelectronics*, 26 (2011) 4585
5. J. Qian, Y. Liu, H. Liu, T. Yu and J. Deng, *Biosensors and Bioelectronics*, 12 (1997) 1213
6. B. Krajewska, *Enzyme and microbial technology*, 35 (2004) 126
7. S. Guo, J. Li, W. Ren, D. Wen, S. Dong and E. Wang, *Chemistry of Materials*, 21 (2009) 2247
8. L. Fu, M.M. Sokiransky, J. Wang, G. Lai and A. Yu, *Physica. E*, 83 (2016) 146
9. Y. Sun and Y. Xia, *Science*, 298 (2002) 2176
10. L. Fu, J. Yong, G. Lai, T. Tamanna, S. Notley and A. Yu, *Materials and Manufacturing Processes*, 29 (2014) 1030
11. Z.-Q. Tian, B. Ren and D.-Y. Wu, *J Phys Chem B*, 106 (2002) 9463
12. L. He, L. Fu and Y. Tang, *Catalysis Science & Technology*, 5 (2015) 1115
13. F.W. Campbell, S.R. Belding, R. Baron, L. Xiao and R.G. Compton, *J Phys Chem C*, 113 (2009) 9053
14. S.E. Ward Jones, F.W. Campbell, R. Baron, L. Xiao and R.G. Compton, *J Phys Chem C*, 112

(2008) 17820
15. P. Ma, H. Zhu, J. Wei and M. Zhang, *Nanoscience and Nanotechnology Letters*, 7 (2015) 127
16. S. Kazemi, B. Hosseinzadeh and S. Zakavi, *Sensors and Actuators B: Chemical*, 210 (2015) 343
17. L. Ding and B. Su, *Journal of Electroanalytical Chemistry*, 736 (2015) 83
18. L. Fu, D. Zhu and A. Yu, *Spectrochimica Acta Part A: Molecular and Biomolecular Spectroscopy*, 149 (2015) 396
19. L. Fu and A. Yu, *Nanoscience and Nanotechnology Letters*, 7 (2015) 147
20. J. Li, H. Li, H. Hu, Y. Zhao and Q. Wang, *Optical Materials*, 40 (2015) 49
21. Z. Shahnavaz, F. Lorestani, W.P. Meng and Y. Alias, *Journal of Solid State Electrochemistry*, 19 (2015) 1223
22. X. Bian, X. Lu, E. Jin, L. Kong, W. Zhang and C. Wang, *Talanta*, 81 (2010) 813
23. A.M. Golsheikh, N.M. Huang, H.N. Lim, R. Zakaria and C.-Y. Yin, *Carbon*, 62 (2013) 405
24. K. Schachl, H. Alemu, K. Kalcher, J. Ježkova, I. Švancara and K. Vytřas, *The Analyst*, 122 (1997) 985
25. L.-C. Jiang and W.-D. Zhang, *Biosensors and Bioelectronics*, 25 (2010) 1402
26. Q. Wang and J. Zheng, *Microchim. Acta.*, 169 (2010) 361
27. T.-H. Tsai, T.-W. Chen and S.-M. Chen, *Int J Electrochem Sci*, 6 (2011) 4628
28. W.-L. Zhu, Y. Wang, J. Xuan and J.-R. Zhang, *Journal of nanoscience and nanotechnology*, 11 (2011) 138
29. L. Zhang, Z. Fang, Y. Ni and G. Zhao, *Int. J. Electrochem. Soc*, 4 (2009) 407
30. Y. Lin, X. Cui and L. Li, *Electrochemistry Communications*, 7 (2005) 166
31. G. Eisenberg, *Industrial & Engineering Chemistry Analytical Edition*, 15 (1943) 327